Catalysis Science & Technology

Accepted Manuscript

ROYAL SOCIETY OF CHEMISTRY

www.rsc.org/catalysis

Table of Contents

Valeric acid and valeric biofuels are obtained in high yield by direct hydrogenation of levulinic acid catalyzed by Pt/HMFI under relatively mild conditions (2 or 8 bar H_2, 200 °C) driven by cooperation of metal and support Brønsted acidity.

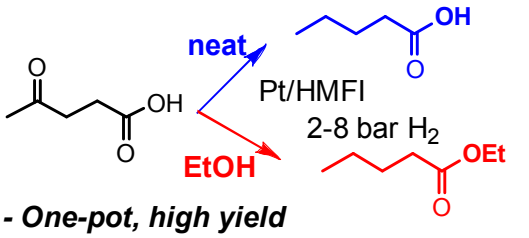

- One-pot, high yield
- Solvent-controlled selectivity switch

Selective hydrogenation of levulinic acid to valeric acid and valeric biofuels by Pt/HMFI catalyst

Kenichi Kon [a], Wataru Onodera,[a] Ken-ichi Shimizu [a,b,*]

[a]Catalysis Research Center, Hokkaido University, N-21, W-10, Sapporo 001-0021, Japan

[b]Elements Strategy Initiative for Catalysts and Batteries, Kyoto University, Katsura, Kyoto 615-8520, Japan

*Corresponding author
Ken-ichi Shimizu
Catalysis Research Center, Hokkaido University, N-21, W-10, Sapporo 001-0021, Japan
E-mail: kshimizu@cat.hokudai.ac.jp, Fax: +81-11-706-9163

Abstract

We describe one-pot high-yield catalytic pathways from levulinic acid (LA) to valeric acid (VA) or valeric acid esters (so called valeric biofuels) under relatively mild conditions (2 or 8 bar H_2, 200 °C). A thorough screening study reveals that HMFI zeolite-supported Pt metal cluster (Pt/HMFI) with average cluster size of 1.9 nm shows the highest yield of VA (99%) under solvent-free conditions. Use of ethanol or methanol as solvent changes the selectivity, resulting in 81-84% yields of ethyl valerate (EV) or methyl valerate (MV). Pt/HMFI is also effective for selective formation of valeric acid esters from γVL in alcohols under H_2. Kinetic, in situ infrared (IR), and acidity-activity relationship studies show cooperative mechanism of Pt and Brønsted acid sites of HMFI. VA formation from LA can be driven by Pt-catalyzed hydrogenation of LA to γVL, which undergoes proton-assisted ring-opening by HMFI, followed by Pt-catalyzed hydrogenation. Valeric esters formation from LA is driven by esterification of LA to levulinic ester, which is hydrogenated by Pt.

Introduction

To achieve sustainable energy production, next-generation biofuels should not compete with food for their feedstock.[1] Levulinic acid (LA) has been identified as a key intermediate in converting non-food biomass into fuels,[1-3] because it can be easily and economically produced from lignocellulosic materials by using a simple hydrolysis process.[2] LA can be converted to derivatives,[1-5] such as ethyl levulinate (EL), γ-valerolactone (γVL), and methyltetrahydrofuran (MTHF), which have been proposed for fuel applications.[6] More promising routes to upgrade LA are the production of valeric acid (VA) and valeric acid esters (so-called valeric or pentanoic biofuels), which has been first proposed by Lange et al.[7] Studies on the fuel properties of the valeric biofuels showed that ethyl valerate (EV) and methyl valerate (MV) have better fuel

performance than current and alternative candidate biofuels (ethanol, n-butanol, EL, γVL, and MTHF).[7,8] The Lange's method is based on gas-phase catalytic reactions using a flow reactor consisted with three steps (Scheme 1): (1) LA hydrogenation to γVL by Pt/TiO_2, followed by (2) γVL hydrogenation to VA by Pt/HMFI zeolite, and by (3) VA esterification to valeric acid esters by acidic resin catalyst. The efficiency of this multi-step process can be improved by process integrations. Lange et al.[7] reported the single-step conversion of γVL to valeric esters over Pt or Pd/TiO_2 catalysts at 275–300 °C under 10 bar, which resulted in 20–50% selectivity of valeric esters. The single-step conversion of LA to EV by co-feeding ethanol with LA over Pt-zeolite lead to co-production of VA and EV, though conversion and selectivity were not reported.[7] γVL can be selectively converted to VA by Pd-NbCe-C catalyst at 325 °C under a flow of 34 bar He/H_2(80/20) with 90% selectivity to VA at 90% conversion.[9] Ravasio et al.[10] reported that hydrogenation of γVL by Cu-based catalyst at 250 °C under 10 bar H_2 gave 59% selectivity to EV at 69% conversion. Recent two reports[11,12] on single-step conversion of LA to VA/EV mixture by acid-metal bifunctional catalysis are more important, because the methods can simplify the process. Weckhuysen et al.[11] showed that hydrogenation of LA by Ru/HMFI at 200 °C under 40 bar H_2 in dioxane resulted in co-production of VA and valeric acid esters with total yield of 45.8%. Fu et al.[12] reported that hydrogenation of LA by Ru/SBA-SO_3H at 240 °C under 40 bar H_2 in ethanol resulted in co-production of VA and EV with total yield of 94%. However, the pioneering methods for direct LA conversion to VA or its esters[7,11,12] suffer from drawbacks of low selectivity (formation of VA/ester mixture) and necessity of high H_2 pressure. We report herein a single-step and highly selective conversion of LA to VA or valeric acid esters by Pt/HMFI catalyst under low H_2 pressure (2 or 8 bar) conditions, in which the selectivity to VA or its esters completely depends on the solvent used. To our knowledge, this is the first example of direct, selective and high-yield production of VA from LA.

Results and Discussion

Characterization of Pt/HMFI

First, we carried out spectroscopic characterizations of the representative catalyst, Pt/HZMFI pre-reduced at 400 °C. The temperature programmed reduction (TPR) profile of the unreduced precursor (Figure S1 in the Supporting information) shows that the reduction of oxidic Pt to metallic Pt occurs below 400 °C. Figure 1A and 1B show X-ray absorption near-edge structures (XANES) and extended X-ray absorption fine structure (EXAFS) of Pt/HMFI and a reference compound (Pt foil). The XANES spectrum of Pt/HMFI is nearly identical to that of Pt foil, which indicates that the electronic state of the Pt species in Pt/HMFI is metallic. This is consistent with the EXAFS analysis (Table 1), which shows only a Pt-Pt contribution of Pt metal at the distance of 2.74 Å. The coordination number (9.6) lower than that of bulk Pt (12)

suggests small size of metallic Pt. Figure S2 shows size distribution of Pt particles observed on the outer surface of Pt/HMF by transmission electron microscopy (TEM). The mean diameter estimated by TEM analysis (4.9 ± 1.4 nm) is larger than that by the CO adsorption experiment (1.9 nm). Considering that small Pt clusters inside zeolite can not be observed by TEM, the results suggest that small Pt clusters are present inside the micropore of HMFI zeolite. IR spectroscopy with CO as a probe molecule allows monitoring of the electronic state of Pt surface. As shown in Figure S3, the IR spectra of CO adsorbed on Pt/HMFI showed a band at 2090 cm^{-1} assignable to linearly coordinated CO on a metallic Pt^0 atom.[13] A band due to bridged CO adspecies on plane sites (1845 cm^{-1})[13] is weak in intensity, which is characteristic to small Pt clusters. Summarizing the structural results, it is concluded that the dominant Pt species in Pt/HFMI are 1.9 nm sized Pt metal clusters.

Direct and selective synthesis of VA

We studied the influence of various catalyst parameters on the catalytic activity for the selective hydrogenation of LA to VA under 8 bar H_2 at 200 ˚C for 1 h using 0.5 mol% of the catalyst under solvent-free conditions (Table 2). First, various metal (M)-loaded HMFI catalysts (M = Pt, Ir, Re, Ag, Pd, Rh, Ru, Cu, Ni, Co) pre-reduced at 400°C were studied (entries 2-11). It was found that Pt/HMFI (entry 2) showed the highest yield of VA (78%). Next, we tested a series of Pt catalysts supported on different materials (entries 2,12-20). Zeolites as Brønsted acidic support (entries 2, 12) gave relatively high yield of VA, and Pt/HMFI showed higher yield (78%) than Pt/HBEA (27%). In contrast, Pt supported on the other oxides with Lewis acidic, neutral, amphoteric or basic nature and carbon-supported Pt as a commercial Pt catalyst selectively produced γVL but did not produce VA except for Pt/SiO_2 which showed low yield of VA (4%). HMFI was completely inactive. Physical mixture of 20 mg of Pt/SiO_2 (0.5 mol% Pt) and 20 mg of HMFI (entry 21) showed lower yield of VA (27%) than Pt/HMFI. These results indicate that Pt metal clusters and the zeolite support itself do not catalyze the selective hydrogenation of LA to VA, and Pt cluster located on and inside HMFI zeolite is responsible for the selective formation of VA.

With the most effective catalyst, Pt/HMFI, we studied the optimization of reaction conditions. Figure 2 shows the effect of hydrogen pressure on the yields of VA and γVL for LA reduction by 0.5 mol% of Pt/HMFI. The VA yield was high in a H_2 pressure range of 8-20 bar. It is important to note that this system is effective even under low H_2 pressure (2 bar). Next, we tested the reaction under 8 bar H_2 for 6 h in different solvents (Table 3). The reaction in toluene, mesitylene, and water gave good yield of VA (73-83%), but dioxane was less effective solvent. The reaction under neat condition (without solvent) gave the highest yield of VA (99%). Under the neat condition, the reaction at lower temperature (150 °C) resulted in the formation of γVL as the main product with VA as minor product (13% yield). Figure 3 shows the time course of

the reaction under neat condition at 200 °C. The profile is characteristic to consecutive reaction mechanism; γVL intermediate, formed at an initial period, was consumed after 0.5 h to give the final product, VA. The maximum yield of VA (99%) was obtained after 6 h, but further increase in the reaction time (10 h) decreased the VA yield. GC analysis of the reaction mixture after 10 h did not show the formation of pentanol and pentanal. Hence, the decrease in the VA yield might be due to its conversion to gas phase hydrocarbons. From the above optimization experiments, we found the best conditions (8 bar H_2, 6 h, 200 °C, 0.5 mol% Pt/HMFI, without solvent), which gave the VA yield of 99% without any byproducts. The turnover frequency (TOF) with respect to all Pt atoms in the Pt/HMFI catalyst corresponds to 33 h^{-1}. Under the similar conditions, we carried out a gram scale reaction experiment; under 10 bar H_2 at 200 °C in the presence of 0.5 mol% Pt/HMFI, 10 mmol (1.161 g) of LA was quantitatively converted to VA after 24 h. This indicates that the method can be applicable to large scale VA production. The longer reaction time (24 h) than the 1 mmol scale experiment (6 h) in Figure 3 might be due to the smaller amount of H_2 (10 bar) per LA (10 mmol) than that for the 1 mmol scale experiment: H_2 (8 bar) per LA (1 mmol).

Under the standard (1 mmol scale) conditions, the reaction was completely terminated by removal of the catalyst from the reaction mixture after 1 h; further heating of the filtrate under 8 bar H_2 for 5 h at 200 °C did not increase the yield. ICP-AES analysis of the filtrate confirmed that the Pt content in the solution was below the detection limit. These results confirm that the reaction is attributed to the heterogeneous catalysis of Pt/HMFI. After the standard reaction for 6 h, the catalyst was separated from reaction mixture by centrifugation and was dried at 90 ºC for 3 h and then reduced in H_2 at 400 ºC for 0.5 h. The recovered catalyst showed nearly quantitative yield of VA (Table 3). However, the catalytic test for the third cycle gave 52% yield of VA. The result of CO adsorption experiment on the Pt/HMFI after the third cycle showed the average Pt particle size of 6.8 nm, which was larger than that of fresh Pt/HMFI (1.9 nm). This indicates that the sintering of Pt clusters is responsible for the decrease in the activity. ICP-AES analysis of the filtrate after the reaction showed Al content of 28 ppm, indicating dealumination during the reaction as pointed out previously.[11] The dealumination could decrease the interaction between the HMFI support and Pt cluster, resulting in the sintering of Pt. The dealumination also decreases the number of Brønsted acid site as a co-catalyst as discussed below.

One-pot synthesis of valeric biofuels

Lange et al.[7] reported the production of valeric acid esters (valeric biofuels) by the three-steps of (1) LA hydrogenation to γVL, (2) γVL hydrogenation to VA, and (3) VA esterification to pentanoic acid esters (Scheme 1). Among valeric acid esters, ethyl valerate (EV) and methyl

valerate (MV) are especially important biofuels.[7,8] To improve the efficiency for pentanoic acid esters formation from LA, we studied one-pot synthesis of EV and MV from LA and alcohols under H_2. Figure 4 shows the time course of the one-pot synthesis of EV from LA in ethanol under 2 bar H_2 at 200 °C. The profile is characteristic to consecutive reaction mechanism; ethyl levulinate (EL) intermediate, formed at an initial induction period, was consumed after 3 h to give its hydrogenated product, EV. Small amounts of VA and methyltetrahydrofuran (MTHF) were also observed as byproducts. After 24 h, the yield of EV reached 75% with 8% VA as a byproduct (eq. 1). The reaction under different H_2 pressure showed that H_2 pressure of 2 bar is optimum. Under the similar reaction conditions, MV was obtained in 87% yield from the one-pot reaction of LA in methanol under 8 bar H_2 (eq. 2). In addition, the same methodology was also effective for selective formation of EV from γVL in ethanol under 2 bar H_2 (eq. 3) and formation of MV from γVL in methanol under 8 bar H_2 (eq. 4).

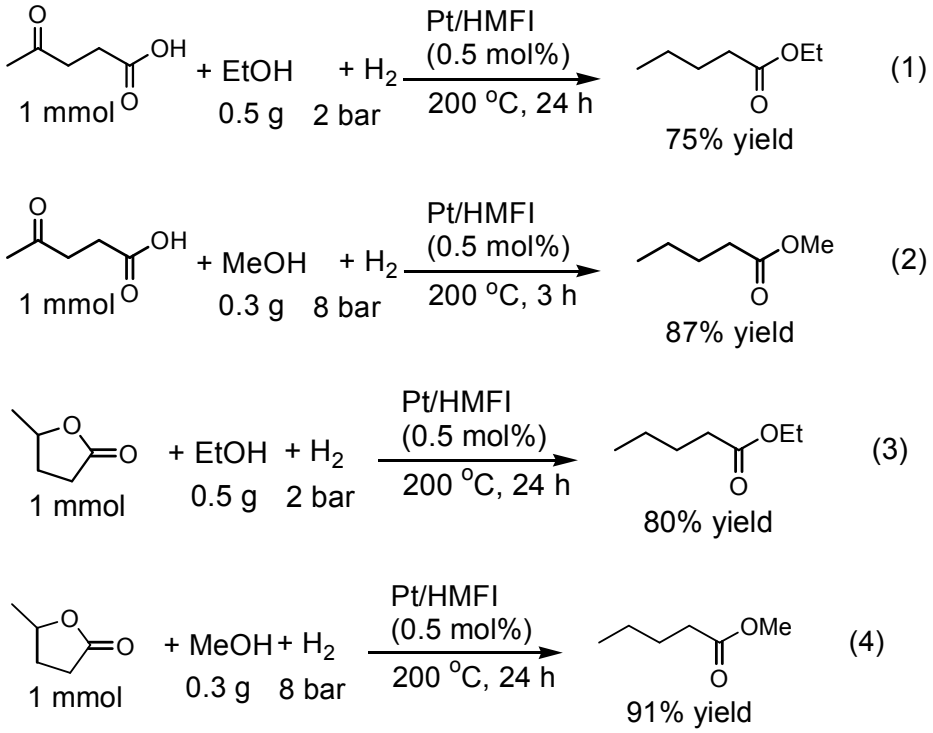

Role of Brønsted acidity in the catalytic pathways

Next, we discuss the effect of support acidity on the catalytic activity and selectivity for LA reduction to VA and valeric esters. On the basis of the well-known classification of support acidity, we chose HMFI, TiO_2 and SiO_2 as model materials of Brønsted acidic, Lewis acidic and nearly neutral supports, respectively. To confirm this classification, we studied pyridine-adsorption IR experiments on these metal oxides. The spectrum of pyridine adsorbed on HMFI (Figure 5A) shows a strong peak at 1543 cm^{-1} due to Brønsted acid sites[14] but no peak due to Lewis acid sites. In contrast, the spectrum for TiO_2 shows a peak at 1444 cm^{-1} due to

Lewis acid sites.[14] These peaks are nearly absent in the spectrum for SiO_2. These results confirmed the above classification of support acidity. Then, we discuss the relationship between the support acidity and catalytic properties of Pt/HMFI, Pt/TiO_2 and Pt/SiO_2 for five reactions shown in Table 4: (I) hydrogenation of LA to VA and γVL, (II) hydrogenation of γVL to VA, (III) hydrogenation of LA to MV in methanol, (VI) hydrogenation of LA to EV in ethanol, (V) esterification of LA to EL in ethanol. Yields of the main products for these reactions are shown in Table 4. For the reaction I, the VA/γVL ratio of the products depended on the acidic nature of the support, and the Brønsted acidic support gave higher VA/γVL ratio than Lewis acidic or neutral support. As shown by the kinetic result in Figure 3, the reaction II is the second step of the reaction I. Table 4 shows that the Brønsted acidic support gives higher activity for γVL reduction to VA (reaction II) than Lewis acidic or neutral support. To further discuss the origin of this support effect, we studied γVL-adsorption IR experiments using HMFI, TiO_2 and SiO_2. As shown in Figure 5B, three or four peaks were observed in the region of stretching vibration of lactone or acid carbonyl group. Considering the fact that liquid γVL shows a single peak due to carbonyl stretching at 1768 cm^{-1},[15] the result indicates acid-base or hydrogen-bonding interaction between support surface and adsorbed γVL. For SiO_2, the main peak at 1764 cm^{-1} is assignable to physically adsorbed γVL. Considering a weakly acidic nature of SiOH groups on amorphous SiO_2 and zeolites, the peak around 1740 cm^{-1} may be due to γVL species weakly interacting with SiOH groups. The positions of the lowest wavenumber peaks for each oxide are listed in Table 4. The result shows that the negative shift in the carbonyl stretching vibration band was largest for HMFI. As proposed by Dumesic et al., protonation of γVL is the initial step of the Brønsted acid-catalyzed ring-opening of γVL to pentenoic acid.[16,17] Taking into account that the peak position (1680 cm^{-1}) for HMFI is in the region of acid carbonyl groups, it is suggested that the reaction of γVL with Brønsted acid site of HMFI leads to ring-opening of γVL according to the mechanism (eq. 5) proposed by Dumesic et al.[16,17]

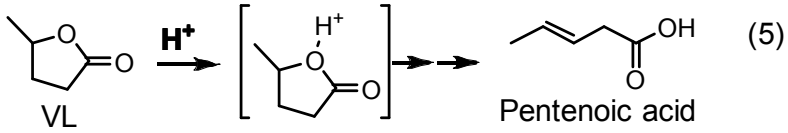

(5)

This mechanism accounts for the Brønsted acid-promoted transformation of γVL to VA (reaction II in Table 4). As reaction I includes the reaction II as the second step, eq. 5 also accounts for the Brønsted acid-promoted transformation of LA to VA (reaction I in Table 4). Based on the above discussion, a mechanism for Pt/HMFI-catalyzed selective hydrogenation of LA to VA is given in Scheme 2. The reaction begins with hydrogenation of LA by Pt sites to γVL, which undergoes ring-opening by Brønsted acid of HMFI to give pentenoic acid. This intermediate is hydrogenated by Pt sites to yield VA. If the ring-opening site (Brønsted acid) is not near the hydrogenation site (Pt), the pentenoic acid as an intermediate could undergo

polymerization. This is a possible reason why the physical mixture of Pt/SiO_2 and HMFI gives lower yield than Pt/HMFI (Table 2).

Next, we discuss the role of Brønsted acid sites in one-pot formation of valeric esters from LA and alcohols by Pt/HFI. As shown in Table 4 (reactions III and IV), hydrogenation of LA to MV (or EV) in methanol (or ethanol) are also support-specific reactions. Brønsted acidic support, HMFI, gave high yields, while Lewis acidic or neutral support resulted in no formation of valeric esters. As shown by the kinetic result in Figure 4, esterification of LA to EL with ethanol (reaction V) is the first step of the one-pot EV formation (reaction IV). Table 4 shows that Pt/HMFI has higher activity for the esterification of LA to EL than TiO_2 and SiO_2 possibly due to the Brønsted acidity of HMFI support. This can account for the high activity of Pt/HMFI for the one-pot formation of valeric esters from LA. The pathway of this system is shown in Scheme 3. The reaction begins with esterification of LA by Brønsted acid of HMFI to give EL, which is hydrogenated by Pt sites to yield valeric esters. These systems represent new examples of heterogeneous bifunctional catalysis driven by cooperative mechanism of metal and Brønsted acid sites.[18]

Finally, we discuss a possible reason why Pt/HMFI gave higher VA yield (78%) from LA than other platinum-group-metal catalysts (Table 2): Ir/HMFI (29%), Pd/HMFI (5%), Rh/HMFI (17%) and Ru/HMFI (30%). As a model reaction of the initial reaction step, LA reduction to γVL, we carried out LA reduction to γVL in milder conditions (2 bar H_2, 80 °C, 0.5 h) than those for LA reduction to VA (8 bar H_2, 200 °C, 1 h). As a model reaction of the second step, γVL reduction to VA, we carried out γVL reduction to VA in 8 bar H_2 at 180 °C. These model reactions were carried out using Pt, Ir, Pd, Rh, or Ru-loaded HMFI under the conditions where conversions were below 32%. The yields are plotted in Fig. 6 as a function of the d-band center (ε_d) relative to the Fermi energy (E_F), ε_d - E_F, for the clean metal surface computed by Hammer and Norskov.[19] Toulhoat and Raybaud reported that bond strength between a metal surface and an hydrogen atom is weaker for a metal with lower ε_d - E_F value.[20] Considering that dissociation of H_2 is usually very fast in a hydrogenation reactions on platinum-group-metal catalysts, the result in Fig. 6 suggests that the less stable M–H bond of the Pt catalyst than the other catalysts leads to the higher rate of H-transfer to unsaturated intermediates in the reactions, resulting in the higher activity for these elementary reactions. This tendency has been observed for several catalytic systems.[20,21]

Conclusions

We have found that VA and valeric acid esters are obtained in high yield (76-99%) by one-pot and one-step hydrogenation catalyzed by Pt/HMFI under relatively mild conditions (2 or 8 bar H_2, 200 °C). Under solvent-free conditions, LA was converted to VA, while in the presence of

alcohols (methanol or ethanol) the selectivity switches from VA to valeric acid esters. Pt/HMFI was also effective for selective hydrogenation of γVL into valeric acid esters in alcohols. The catalytic system is driven by cooperative mechanism of Pt and Brønsted acid sites of HMFI. VA formation from LA is driven by Pt-catalyzed hydrogenation of LA to γVL, which undergoes protonation and ring-opening by HMFI and subsequent hydrogenation by Pt. Valeric esters formation from LA is driven by the first esterification of LA, followed by Pt-catalyzed hydrogenation of levulinic esters. The above catalytic systems can provide sustainable pathways to biofuels from non-food biomass-derived LA, because the catalyst, readily prepared from commercial materials, shows high yields under mild conditions.

Experimental

Catalyst preparation

H^+-type MFI zeolite (HMFI) with a SiO_2/Al_2O_3 ratio of 22.3 was kindly supplied by Tosoh Co. Montmorillonite K10 clay was purchased from Sigma-Aldrich. SiO_2 (Q-10, 300 m^2 g^{-1}) was supplied from Fuji Silysia Chemical Ltd. HBEA zeolite (JRC-Z-HB25, SiO_2/Al_2O_3= 25±5), MgO (JRC-MGO-3), TiO_2 (JRC-TIO-4), CeO_2 (JRC-CEO-3) was supplied from Catalysis Society of Japan. γ-Al_2O_3 was prepared by calcination of γ-AlOOH (Catapal B Alumina purchased from Sasol) for 3 h at 900 °C. Nb_2O_5 was prepared by calcination of $Nb_2O_5 \cdot nH_2O$ (supplied by CBMM) at 500 °C for 3 h.

Precursor of Pt/HMFI was prepared by impregnation method; a mixture of HMFI and an aqueous HNO_3 solution of $Pt(NH_3)_2(NO_3)_2$ was evaporated at 50 °C, followed by drying at 90 °C for 12 h. Before catalytic and characterization experiments, the Pt/HMFI catalyst (with Pt loading of 5 wt%) was prepared by in situ pre-reduction of the precursor in a pyrex tube under a flow of H_2 (20 cm^3 min^{-1}) at 400 °C for 0.5 h. Other supported Pt catalysts were prepared by the same method. HMFI–supported metal catalysts, M/HMFI (M = Co, Ni, Cu, Ru, Rh, Pd, Ag, Re, Ir) with metal loading of 5 wt% were prepared by impregnation method in the similar manner as Pt/HMFI using aqueous solution of metal nitrates (for Co, Ni, Cu, Ag), $RuCl_3$, $IrCl_3 \cdot nH_2O$, NH_4ReO_4 or aqueous HNO_3 solution of $Rh(NO_3)_3$ or $Pd(NO_3)_2$. Pt/C was purchased from N.E. CHEMCAT.

Characterization

H_2-TPR was carried out with BELCAT (BELL Japan Inc.). Unreduced precursor of Pt/HMFI, $Pt(NH_3)_2(NO_3)_2$-loaded HMFI (20 mg), was mounted in a quartz tube, and the sample was heated with a temperature ramp-rate of 10 °C min^{-1} in a flow of 5% H_2/Ar (20 cm^3 min^{-1}). The effluent gas was passed through a trap containing MS4Å to remove water, then through the thermal conductivity detector. The amount of H_2 consumed during the experiment was detected by a thermal conductivity detector.

The number of surface metal atoms in Pt/HMFI, pre-reduced in H_2 at 400 °C, was estimated from the CO uptake of the samples at room temperature using the pulse-adsorption of CO in a flow of He by BELCAT. The average particle size was calculated from the CO uptake assuming that CO was adsorbed on the surface of spherical Pt particles at CO/(surface Pt atom) = 1/1 stoichiometry.

TEM measurements were carried out by using a JEOL JEM-2100F TEM operated at 200 kV.

XANES and EXAFS at Pt L_3-edge were measured at the BL14B2 in the SPring-8 (Proposal No. 2012A1734) in a transmittance mode. The storage ring was operated at 8 GeV. A Si(111) single crystal was used to obtain a monochromatic X-ray beam. The Pt/HMFI pre-reduced in 100% H_2 (20 cm^3 min^{-1}) for 0.5 h at 400 °C was cooled to room temperature in the flow of H_2 and was sealed in cells made of polyethylene under N_2, and then the spectrum was taken at room temperature. The EXAFS analysis was performed using the REX version 2.5 program (RIGAKU). The parameters for the Pt–Pt shell were provided by the FEFF6.

In situ IR spectra were recorded at 40 °C using a JASCO FT/IR-4200 equipped with a quartz IR cell connected to a conventional flow reaction system. The sample was pressed into a 30 mg of self-supporting wafer (ϕ = 2 cm) and mounted into the quartz IR cell with CaF_2 windows. Spectra were measured accumulating 30 scans at a resolution of 4 cm^{-1}. A reference spectrum of the catalyst wafer in He taken at measurement temperature was subtracted from each spectrum. Prior to the experiment the disk of Pt/HMFI was heated in H_2 flow (20 cm^3 min^{-1}) at 400 °C for 0.5 h, followed by cooling to 40 °C and purging with He. Then, the catalyst was exposed to a flow of CO(5%)/He (20 cm^3 min^{-1}) for 180 s, followed by purging with He for 600 s. For the IR measurements of pyridine and γVL on metal oxides at150 °C, the liquid compound was injected to He flow preheated at 200 °C, which was fed to the IR cell. Then, the IR disk was purged with He for 200 s, and IR measurement was carried out.

Catalytic tests

Commercially available organic compounds (from Tokyo Chemical Industry) were used without further purification. Typically, Pt/HMFI (0.5 mol% with respect to levulinic acid) pre-reduced at 400 °C was used as a standard catalyst. After the pre-reduction, the catalyst in the closed glass tube sealed with a septum inlet was cooled to room temperature under H_2 atmosphere. The mixture of levulinic acid (1 mmol, 116.1 mg, 0.102 cm^3) and *n*-dodecane (0.5 mmol, 85.2 mg, 0.114 cm^3) as internal standard was injected to the pre-reduced catalyst inside the glass tube through the septum inlet. Then, the septum was removed under air, and a magnetic stirrer was put in the tube, followed by inserting the tube inside stainless autoclave with a dead space of 33 cm^3. Soon after being sealed, the reactor was flushed with H_2 from a high pressure gas cylinder and charged with 2 or 8 bar H_2 at room temperature. Then, the reactor was heated at 200 ˚C under stirring (400 rpm). Conversion and yields of products were determined by GC (Shimadzu

GC-14B, N_2 as the carrier gas) equipped with Ultra ALLOY capillary column UA^+-5 (Frontier Laboratories Ltd.) using *n*-dodecane as an internal standard. The products were identified by GC-MS (Shimadzu GCMS-QP2010, He as the carrier gas) equipped with the same column as GC and by comparison with commercially pure products. For the data in Table 4, we carried out three catalytic tests to show averaged GC yields. For other data yield for a single reaction is shown.

Acknowledgement

This work was supported by a Grant-in-Aid for Scientific Research on Innovative Areas "Nano Informatics" (25106010) from JSPS and a MEXT program "Elements Strategy Initiative to Form Core Research Center".

References

1 M. J. Climent, A. Corma and S. Iborra, *Green Chem.*, 2014, **16**, 516–547.

2 (a) G. W. Huber, S. Iborra and A. Corma, *Chem. Rev.*, 2006, **106**, 4044–4048; (b) D. W. Rackemann and W. O. S. Doherty, *Biofuels Bioprod. Biorefin.* 2011, **5**, 198–214; (c) G. Novodárszki, N. Rétfalvi, G. Dibó, P. Mizsey, E. Cséfalvay and L. T. Mika, *RSC Adv.*, 2014, **4**, 2081–2088; (d) P. A. Son, S. Nishimura and K. Ebitani, *React. Kinet., Mech. Catal.*, 2014, **111**, 183–197; (e) P. A. Son, S. Nishimura and K. Ebitani, *React. Kinet., Mech. Catal.*, 2012, **106**, 185–192.

3 (a) D. M. Alonso, S. G. Wettstein and J. A. Dumesic, *Green Chem.*, 2013, **15**, 584–595; (b) W. R. H. Wright and R. Palkovits, *ChemSusChem*, 2012, **5**, 1657–1667.

4 (a) A. M. R. Galletti, C. Antonetti, V. D. Luise and M. Martinelli, *Green Chem.*, 2012, **14**, 688–694; (b) V. Mohan, C. Raghavendra, C. V. Pramod, B. D. Raju and K. S. R. Rao, *RSC Adv.*, 2014, **4**, 9660–9668; (c) V. Mohan, V. Venkateshwarlu, C. V. Pramod, B. D. Raju and K. S. R. Rao, *Catal. Sci. Technol.*, 2014, **4**, 1253–1259.

5 (a) L. Deng, J. Li, D. M. Lai, Y. Fu and Q. X. Guo, *Angew. Chem. Int. Ed.*, 2009, **48**, 6529–6532; (b) J. Deng, Y. Wang, T. Pan, Q. Xu, Q. X. Guo and Y. Fu, *ChemSusChem*, 2013, **6**, 1163–1167; (c) X. L. Du, L. He, S. Zhao, Y. M. Liu, Y. Cao, H. Y. He and K. N. Fan, *Angew. Chem., Int. Ed.*, 2011, 50, 7815–7819; (d) A. M. Hengne, A. V. Malawadkar, N. S. Biradar and C. V. Rode, *RSC Adv.*, 2014, **4**, 9730–9736; (e) P. A. Son, S. Nishimura and K. Ebitani, *RSC Adv.*, 2014, **4**, 10525–10530.

6 I. T. Horváth, H. Mehdi, V. Fábos, L. Boda and L. T. Mika, *Green Chem.*, 2008, **10**, 238–242.

7 J.-P. Lange, R. Price, P.M. Ayoub, J. Louis, L. Petrus, L. Clarke and H. Gosselink, *Angew. Chem. Int. Ed.*, 2010, **49**, 4479–4483.

8 G. Dayma, F. Halter, F. Foucher, C. Togbé, C. Mounaim-Rousselle and P. Dagaut, *Energy Fuels*, 2012, **26**, 4735–4748.

9 D. J. Braden, C. A. Henao, J. Heltzel, C. C. Maravelias and J. A. Dumesic, *Green Chem.*, 2011, **13**, 1755–3324.

10 C. E. Chan-Thaw, M. Marelli, R. Psaro, N. Ravasio and F. Zaccheria, *RSC Adv.*, 2013, **3**, 1302–1306.

11 W. H. Luo, U. Deka, A. M. Beale, E. R. H. van Eck, P. C. A. Bruijnincx and B. M. Weckhuysen, *J. Catal.*, 2013, **301**, 175–186.

12 Tao Pan, Jin Deng, Qing Xu, Yang Xu, Qing-Xiang Guo and Yao Fu, *Green Chem.*, 2013, **15**, 2967–2974

13 J. Raskó, *J. Catal.*, 2003, **217**, 478–486.

14 M. Tamura, K. Shimizu and A. Satsuma, *Appl. Catal. A*, 2012, **433–434**, 135–145.

15 J. M. Tukacs, D. Király, A. Strádi, G. Novodarszki, Z. Eke, G. Dibó, T. Kégl and L. T. Mika, *Green Chem.*, 2012, **14**, 2057–2065.

16 J. Q. Bond, D. M. Alonso, R. M. West and J. A. Dumesic, *Langmuir*, 2010, **26**, 16291–16298.

17 J. Q. Bond, D. Wang, D. M. Alonso and J. A. Dumesic, *J. Catal.*, 2011, **281**, 290–299.

18 P. Barbaro, F. Liguori, N. Linares and C. M. Marrodan, *Eur. J. Inorg. Chem.*, **2012**, 3807–3823.

19 B. Hammer and J. K. Norskov, *Adv. Catal.*, **45**, 71–129.

20 H. Toulhoat and P. Raybaud, *J. Catal.*, 2003, **216**, 63–72.

21 M. Tamura, K. Kon, A. Satsuma and K. Shimizu, *ACS Catal.* 2012, **2**, 1904–1909.

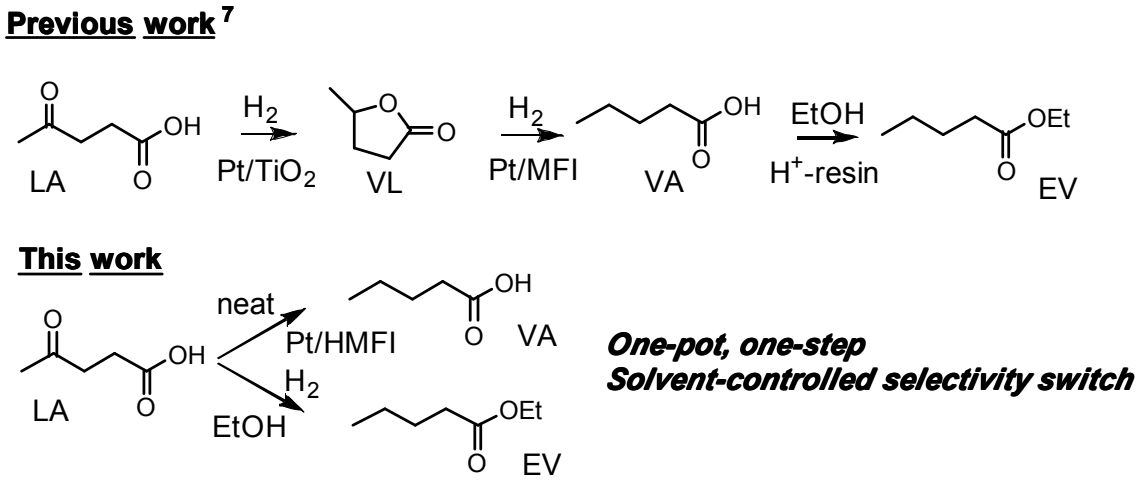

Scheme 1 Three-steps and one-step transformations of LA to valeric biofuels.

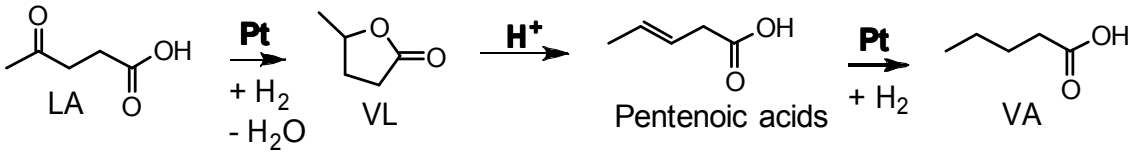

Scheme 2 Proposed pathway of one-pot LA reduction to VA promoted by Brønsted acid site.

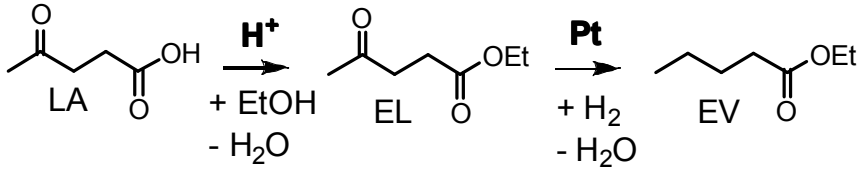

Scheme 3 Proposed pathway of one-pot LA reduction to EV promoted by Brønsted acid site.

Table 1 Curve-fitting analysis of Pt L_3-edge EXAFS.

Sample	Shell	N [a]	*R*/Å [b]	σ /Å [c]	R_f /% [d]
Pt/HMFI	Pt	9.6	2.74	0.076	2.4
Pt metal[e]	Pt	12	2.76	-	-

[a] Coordination numbers. [b] Bond distance. [c] Debye-Waller factor. [d] Residual factor.

[e] Crystallographic data of Pt metal.

Table 2 Hydrogenation of levulinic acid.[a]

Entry	Catalyst	Conv. (%)	VA yield (%)	γVL yield (%)
1	HMFI	26	0	0
2	Pt/HMFI	100	78	15
3	Ir/HMFI	100	29	48
4	Re/HMFI	22	0	4
5	Ag/HMFI	6	0	4
6	Pd/HMFI	92	5	47
7	Rh/HMFI	100	17	60
8	Ru/HMFI	100	30	59
9	Cu/HMFI	8	0	0
10	Ni/HMFI	6	0	4
11	Co/HMFI	6	0	0
12	Pt/HBEA	100	27	51
13	Pt/Al_2O_3	100	0	54
14	Pt/Nb_2O_5	100	0	75
15	Pt/K10-clay	100	0	80
16	Pt/TiO_2	100	1	75
17	Pt/SiO_2	100	4	92
18	Pt/carbon	100	0	14
19	Pt/CeO_2	100	0	26
20	Pt/MgO	100	0	72
21	Pt/SiO_2+HMFI	100	23	50

[a] Conditions: neat LA (1 mmol), catalyst (0.5 mol%), 200 °C, 8 bar H_2, 1 h. Yields of VA and γVL were determined by GC.

Table 3 Solvent effect in hydrogenation of LA by Pt/HMFI.[a]

Solvent	*T* (°C)	Conv. (%)	VA yield (%)	γVL yield (%)
toluene	200	100	83	0
mesitylene	200	100	81	0
dioxane	200	100	19	40
water	200	100	73	0
solvent-free	150	100	13	68
solvent-free	200	100	99	0
solvent-free [b]	200 [b]	100 [b]	99 [b]	0 [b]
solvent-free [c]	200 [c]	100 [c]	52 [c]	30 [c]

[a] Conditions: LA (1 mmol), solvent (0 or 0.3 g), catalyst (0.5 mol%), 8 bar H_2, 6 h. Yields of VA and γVL were determined by GC.

[b] Cycle 2.

[c] Cycle 3.

Table 4 Summary of IR results and product yields for Pt-catalyzed reactions I-V.

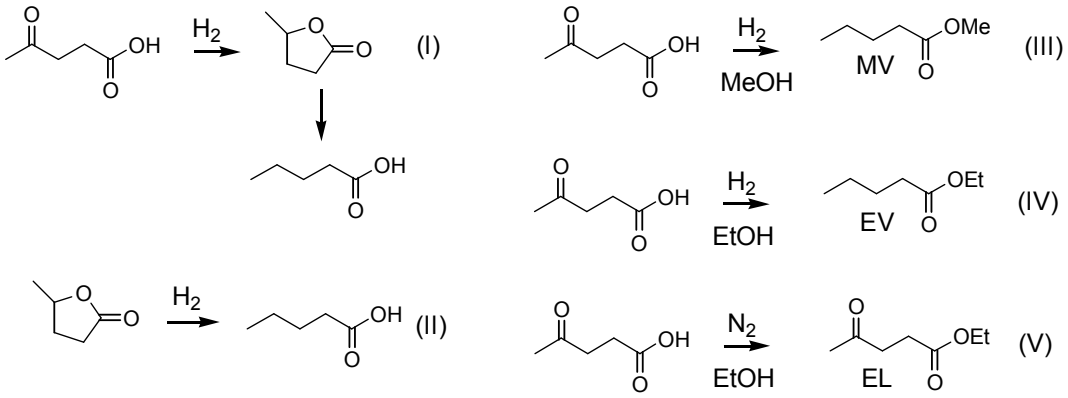

Catalyst	Acidity	IR of γVL ν / cm^{-1}	I[a] VA/γVL (%)	II[b] VA (%)	III [c] MV (%)	IV [d] EV (%)	V[e] EL (%)
Pt/HMFI	Brønsted	1680	78 / 15	76	87	75	96
Pt/TiO_2	Lewis	1703	1 / 75	0	0	0	52
Pt/SiO_2	neutral	1740	4 / 92	0	0	0	50

[a] from Table 2.

[b] Conditions: neat γVL (1 mmol), catalyst (0.5 mol%), 200 °C, 8 bar H_2, 6 h.

[c] Conditions: LA (1 mmol), MeOH (0.3 g), catalyst (0.5 mol%), 200 °C, 8 bar H_2, 24 h.

[d] Conditions: LA (1 mmol), EtOH (0.5 g), catalyst (0.5 mol%), 200 °C, 2 bar H_2, 24 h.

[e] Conditions: LA (1 mmol), EtOH (0.5 g), catalyst 20 mg, 150 °C, 1 bar N_2, 1 h.

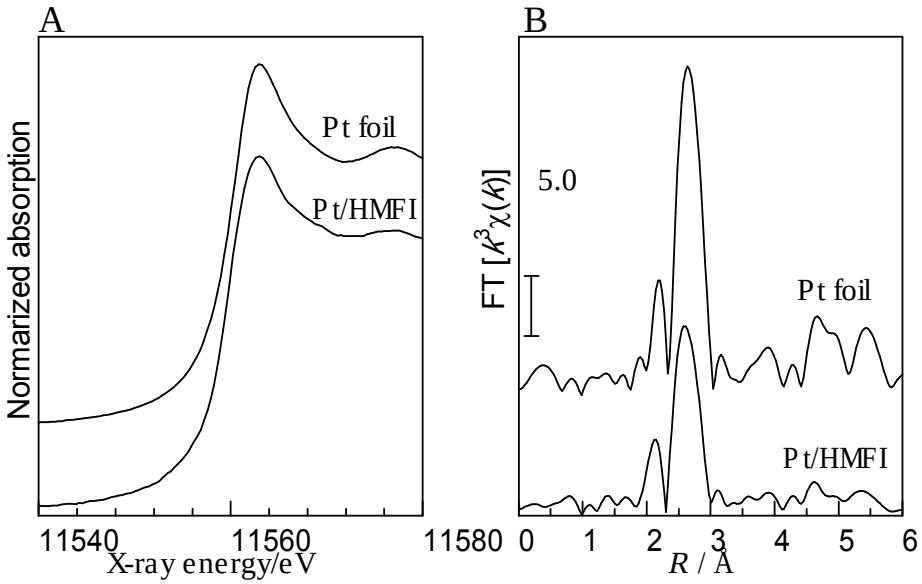

Fig. 1 Pt L_3-edge XANES spectra (A) and EXAFS Fourier transforms (B).

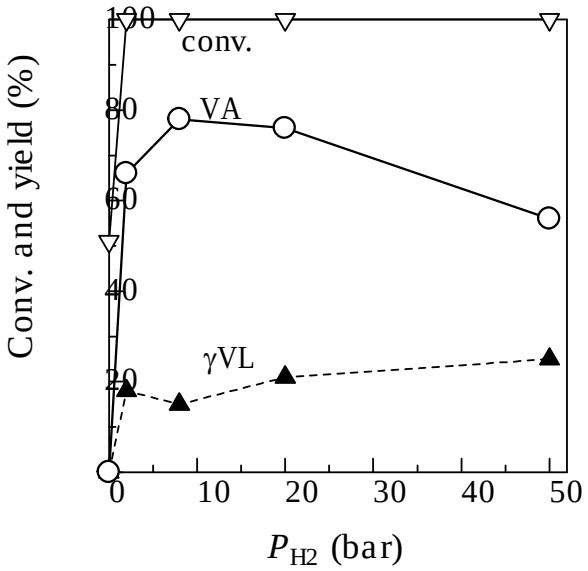

Fig. 2 Effect of hydrogen pressure on conversion (▽) and yields of VA (○) and γVL (▲) for hydrogenation of neat LA by Pt/HMFI (0.5 mol%) at 200 °C for 1 h.

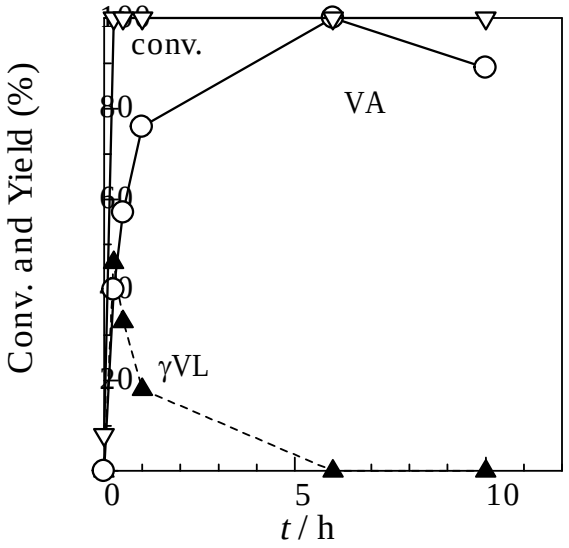

Fig. 3 Conversion of LA (▽) and yields of VA (○) and γVL (▲) for hydrogenation of neat LA by Pt/HMFI (0.5 mol%) at 200 °C under 8 bar H_2.

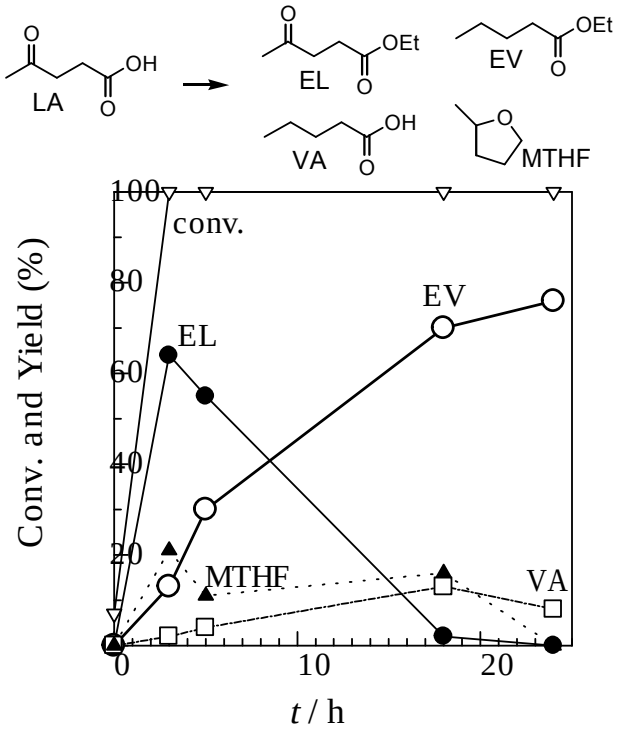

Fig. 4 Conversion of LA (▽) and yields of ethyl levulinate (EL, ●), ethyl valerate (EV, ○), valeric acid (VA, □) and methyltetrahydrofuran (MTHF, ▲) for LA reduction in 0.5 g EtOH under 2 bar H_2 by Pt/HMFI (0.5 mol%) at 200 °C.

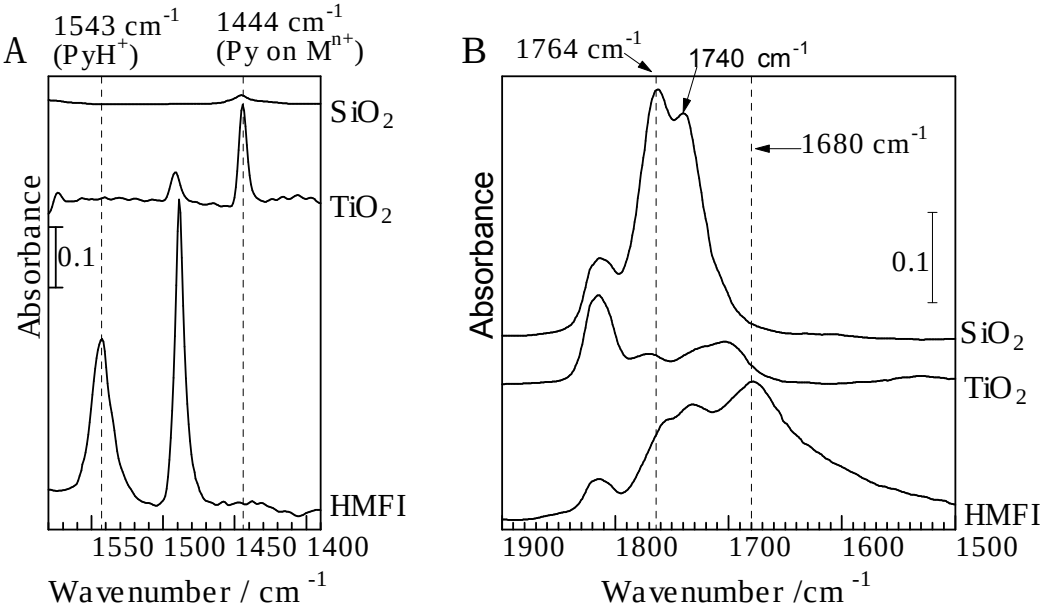

Fig. 5 IR spectra of (A) pyridine and (B) γVL adsorbed on various supports at 150 °C.

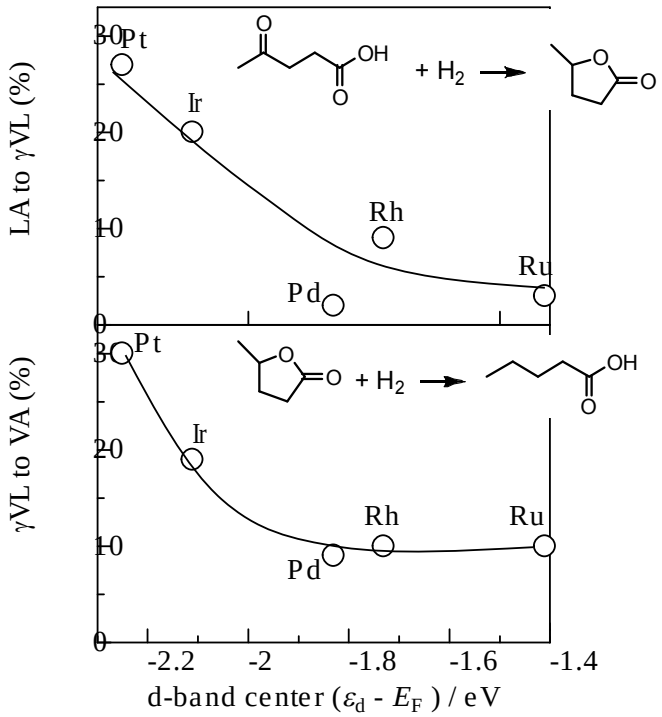

Fig. 6 Effect of the d-band center of metals relative to the Fermi energy (ε_d - E_F) [19] on the yield of the products for model hydrogenation of LA to γVL and γVL to VA by metal-loaded HMFI catalysts under the conditions where conversions were below 32%. Conditions for LA reduction: neat LA (1 mmol), catalyst (0.5 mol%), 80 °C, 2 bar H_2, 0.5 h. Conditions for γVL reduction: neat γVL (1 mmol), catalyst (0.5 mol%), 180 °C, 8 bar H_2, 1 h.